Bi-ionic system: theoretical investigation on the ionic fluxes through an ion-exchange membrane

Sami Mokrani, Lasâad Dammak, Christian Larchet and Bernard Auclair*

Laboratoire des Matériaux Echangeurs d'Ions, Université de Paris-Val de Marne, 94010 Créteil, France. E-mail: lmei@univ-paris12.fr

Received (in Montpellier, France) 21st December 1998, Accepted 12th February 1999

We have established a theoretical description of the co-ion and counter-ion fluxes through an ion-exchange membrane (IEM) used in a bi-ionic system. This study is based on the modified Nernst–Planck equation applied to three parallel homogenous phases: two diffusion boundary layers (DBLs) and an IEM. The role of the IEM and of the DBLs in the control of the interdiffusion process is discussed. The influence of the common concentration, the co-ion and counter-ion diffusion coefficients in the membrane, the membrane selectivity and affinity, the concentration of functional sites and the convection velocity are evaluated.

Système bi-onique: étude théorique des flux ioniques à travers une membrane échangeuse d'ions. Nous avons établi une étude théorique des flux du co-ion et des contre-ions à travers une membrane échangeuse d'ions (MEI) utilisée dans un système bi-ionique. Cette étude est basée sur l'équation modifiée de Nernst–Planck appliquée à trois phases parallèles: deux couches limites de diffusion (CLE) et une MEI. La part de la MEI et des CLE dans le contrôle du processus d'interdiffusion est discutée. L'influence de la concentration commune, des coefficients de diffusion du co-ion et des contre-ions dans la membrane, de la sélectivité et de l'affinité membranaires, de la concentration des sites fonctionnels et de la vitesse de convection sont évalués.

A bi-ionic system (BIS) is constituted of an ion-exchange membrane (IEM) separating two electrolyte solutions having the same co-ion, Y, at the same concentration C_0, but different counter-ions: A and B. It will be denoted as AY (C_0) /IEM/BY(C_0). In this system, we observe an interdiffusion process (IDP) between the two counter-ions, under the influence of their concentration gradients. Quickly, the system will become multi-ionic because the two counter-ions will exist in both compartments. In most papers dealing with bi-ionic systems,[1–9] attention has been focused on potential measurements and/or computations. But the analysis of transmembrane ionic flux has been neglected because of the difficulty of its study.[10] For example Dammak *et al.*[11] have proposed an experimental setup to maintain the system as near as possible to the real state of a BIS and the corresponding measurement protocol for determining the bi-ionic potential (BIP). They have elaborated a theoretical treatment, based on the modified Nernst–Planck equation[12] to interpret their BIP experimental results. They have shown also the suitability of these equations for describing the transport phenomenon through an IEM and the utility of studying this phenomenon over the entire concentration range (10^{-5}–1 M)

For the ion fluxes, we remark that until now, all analytical solutions, giving these through an IEM have been established by several authors[9,10,13] for the two limiting concentration domains only. *Very low concentrations.* One of the concentrations is less than 10^{-2} M; the authors[9–13] have shown that in this case the diffusion boundary layers (DBLs) control completely the IDP. *Very high concentrations.* Both concentrations are higher than 1 M. It has been shown[9] that in this case the IEM controls completely the IDP. However, for the intermediate concentrations, the most used experimentally, there are neither significant theoretical nor experimental studies.

In this paper, we propose to solve the same equations used by Dammak *et al.*[11] in the case of a bi-ionic system in order to study theoretically the transmembrane ionic flux variations over all concentration domains and with different influencing parameters. This approach will be used in the future to develop the study on multi-ionic systems (MIS), considered as the real representation of crossed ionic dialysis (Donnan dialysis).

We have organized this paper as follows. First, we will present a short theoretical development, then we will give the general variation curves of the counter-ion and co-ion fluxes and finally we will evaluate the influence of each parameter taking part in the interdiffusion process.

Theoretical development

The system under study is shown in Fig. 1. It consists of a cation-exchange membrane (CEM), with univalent fixed anions at a total concentration of X, separating two solutions a and b whose compositions are maintained constant in time. In this system we distinguish four different interfaces: (*i*) bulk solution a–DBLa, at $x = -\delta_a$, (*ii*) DBLa–CEM, at $x = 0$, (*iii*) CEM–DBLb, at $x = d$, and (*iv*) DBLb–bulk solution b, at $x = d + \delta_b$. Thermodynamic equilibrium is presumed between the different phases at each interface.[9] The kinetics of ion exchange at the level of the DBL–IEM interfaces is assumed to be instantaneous,[14] thus only the diffusion process will be studied.

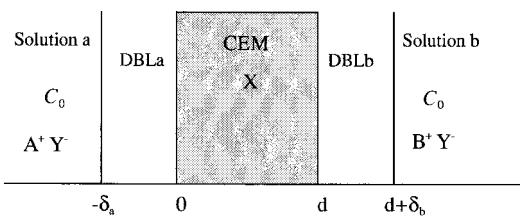

Fig. 1 The study system of the cation-exchange membrane.

Recent studies on the BIP[8,15] lead to the following assumptions, in order to be as close as possible to the real conditions of a BIS: (*i*) mixed control of the interdiffusion process by both the charged membrane and the diffusion boundary layers, (*ii*) the co-ion flux is different from zero, (*iii*) the solvent flux is not nil, (*iv*) the affinity and selectivity coefficients are neither constant nor equal to one, (*v*) the electroneutrality is respected in each phase, and (*vi*) a zero current density through the studied system is considered.

The Nernst–Planck equation is the most frequently used to describe the transport phenomenon of matter in solution and through IEMs. However, this equation does not take into account the solvent flux. We use then the modified Nernst–Planck equation that includes the correction term $C_i V_M$ to calculate the flux J_i of ion i:

$$J_i = -D_i\left\{\nabla(C_i) + C_i\nabla[\mathrm{Ln}(\gamma_i)] + z_i C_i \frac{F}{RT}\nabla(\psi)\right\} + C_i V_M \tag{1}$$

where D_i denotes the diffusion coefficient of the ionic species i, z_i its valence, γ_i its molar activity coefficient, F is Faraday's constant, R is the ideal gas constant and T is the absolute temperature. The ion concentration C_i and the electric potential ψ are assumed to vary only in the x direction. V_M is the solution center-of-mass velocity in the membrane.

In the usual concentration range ($C_0 \approx 1$ mol L^{-1}) and for almost all electrolytes (different from HCl and NaOH) we can suppose $\overline{\gamma_i}$ is constant, but it can be different from unity. In fact, the electrolyte quantity absorbed by the membrane remains negligible compared to X (functional site concentration) in recently developed membranes. Thus, the electrolyte strength in the membrane will be independant of the external concentration. Eqn. (1) for a 1 : 1 electrolyte becomes

$$J_i = -\overline{D_i}\left(\frac{d\overline{C_i}}{dx} + \overline{C_i}\frac{F}{RT}\frac{\overline{d\psi}}{dx}\right) + \overline{C_i} V_M \tag{2}$$

where the bars denotes the membrane phase.

In this part we will describe the mathematical treatment only for the membrane phase. The same treatments may be achieved for the two DBLs, by considering $x = 0$, $x = d$ and removing the bar on the physico-chemical magnitudes. For the three ionic species within the membrane, which is considered as homogeneous,[16] we can write:

$$\overline{J_A} = J_A = -\overline{D_A}\left(\frac{d\overline{C_A}}{dx} + \overline{C_A}\frac{F}{RT}\frac{\overline{d\psi}}{dx}\right) + \overline{C_A} V_M \tag{3a}$$

$$\overline{J_B} = J_B = -\overline{D_B}\left(\frac{d\overline{C_B}}{dx} + \overline{C_B}\frac{F}{RT}\frac{\overline{d\psi}}{dx}\right) + \overline{C_B} V_M \tag{3b}$$

$$\overline{J_Y} = J_Y = -\overline{D_Y}\left(\frac{d\overline{C_Y}}{dx} - \overline{C_Y}\frac{F}{RT}\frac{\overline{d\psi}}{dx}\right) + \overline{C_Y} V_M \tag{3c}$$

The electroneutrality condition and the zero current density condition lead, respectively, to the two equations:

$$\overline{C_A} + \overline{C_B} = \overline{C_Y} + X \tag{4a}$$

$$J_A + J_B = J_Y \tag{4b}$$

Removing the potential gradient from eqn. (3), we obtain:

$$-\frac{J_A}{\overline{D_A}} = \frac{d\overline{C_A}}{dx} + \overline{C_A}\frac{\begin{array}{c}V_M X + [(\overline{D_Y} - \overline{D_A})\, d\overline{C_A}/dx \\ + (\overline{D_Y} - \overline{D_B})\, d\overline{C_B}/dx]\end{array}}{\begin{array}{l}[(\overline{D_Y} + \overline{D_A})\overline{C_A} \\ \quad + (\overline{D_Y} + \overline{D_B})\overline{C_B} - \overline{D_Y} X]\end{array}} - \frac{\overline{C_A}}{\overline{D_A}} V_M \tag{5}$$

For the counter-ion B, we obtain a similar equation by permuting A and B in the last equation. After rearrangements we obtain:

$$\begin{aligned}&-\frac{J_A}{\overline{D_A}}[(\overline{D_Y} + \overline{D_A})\overline{C_A} + (\overline{D_Y} + \overline{D_B})\overline{C_B} - \overline{D_Y} X] \\ &\quad + \frac{\overline{C_A}}{\overline{D_A}} V_M[(\overline{D_Y} + \overline{D_A})(\overline{C_A} - X) + (\overline{D_Y} + \overline{D_B})\overline{C_B}] \\ &= [(2\overline{C_A} + \overline{C_B} - X)\overline{D_Y} + \overline{C_B}\,\overline{D_B}]\frac{d\overline{C_A}}{dx} + \overline{C_A}(\overline{D_Y} - \overline{D_B})\frac{d\overline{C_B}}{dx}\end{aligned} \tag{6a}$$

$$\begin{aligned}&-\frac{J_B}{\overline{D_B}}[(\overline{D_Y} + \overline{D_B})\overline{C_B} + (\overline{D_Y} + \overline{D_A})\overline{C_A} - \overline{D_Y} X] \\ &\quad + \frac{\overline{C_B}}{\overline{D_B}} V_M[(\overline{D_Y} + \overline{D_B})(\overline{C_B} - X) + (\overline{D_Y} + \overline{D_A})\overline{C_A}] \\ &= [(2\overline{C_B} + \overline{C_A} - X)\overline{D_Y} + \overline{C_A}\,\overline{D_A}]\frac{d\overline{C_B}}{dx} + \overline{C_B}(\overline{D_Y} - \overline{D_A})\frac{d\overline{C_A}}{dx}\end{aligned} \tag{6b}$$

If we define:

$$\begin{aligned}\overline{\alpha_{A0}} &= -\frac{J_A}{\overline{D_A}}[(\overline{D_Y} + \overline{D_A})\overline{C_A} + (\overline{D_Y} + \overline{D_B})\overline{C_B} - \overline{D_Y} X] \\ &\quad + \frac{\overline{C_A}}{\overline{D_A}} V_M[(\overline{D_Y} + \overline{D_A})(\overline{C_A} - X) + (\overline{D_Y} + \overline{D_B})\overline{C_B}] \\ \overline{\alpha_{A1}} &= [(2\overline{C_A} + \overline{C_B} - X)\overline{D_Y} + \overline{C_B}\,\overline{D_B}] \\ \overline{\alpha_{A2}} &= \overline{C_A}(\overline{D_Y} - \overline{D_B}) \\ \overline{\alpha_{B0}} &= -\frac{J_B}{\overline{D_B}}[(\overline{D_Y} + \overline{D_B})\overline{C_B} + (\overline{D_Y} + \overline{D_A})\overline{C_A} - \overline{D_Y} X] \\ &\quad + \frac{\overline{C_B}}{\overline{D_B}} V_M[(\overline{D_Y} + \overline{D_B})(\overline{C_B} - X) + (\overline{D_Y} + \overline{D_A})\overline{C_A}] \\ \overline{\alpha_{B1}} &= \overline{C_B}(\overline{D_Y} - \overline{D_A}) \\ \overline{\alpha_{B2}} &= [(2\overline{D_B} + \overline{C_A} - X)\overline{D_Y} + \overline{C_A}\,\overline{D_A}]\end{aligned}$$

Eqn. (6a) and (6b) may be written as:

$$\overline{\alpha_{A0}} = \overline{\alpha_{A1}}\frac{d\overline{C_A}}{dx} + \overline{\alpha_{A2}}\frac{d\overline{C_B}}{dx} \tag{7a}$$

$$\overline{\alpha_{B0}} = \overline{\alpha_{B1}}\frac{d\overline{C_A}}{dx} + \overline{\alpha_{B2}}\frac{d\overline{C_B}}{dx} \tag{7b}$$

We can re-write the system (7a, 7b) in order to give $d\overline{C_A}/dx$ and $d\overline{C_B}/dx$ in the form of two differential equations as a function of the parameters $\overline{D_A}$, $\overline{D_B}$, $\overline{D_Y}$, $\overline{C_A}$, $\overline{C_B}$, X, d and V_M:

$$\begin{aligned}\frac{d\overline{C_A}}{dx} &= \frac{\overline{\alpha_{A0}}\,\overline{\alpha_{B2}} - \overline{\alpha_{B0}}\,\overline{\alpha_{A2}}}{\overline{\alpha_{A1}}\,\overline{\alpha_{B2}} - \overline{\alpha_{B1}}\,\overline{\alpha_{A2}}} \\ &= f(\overline{D_A}, \overline{D_B}, \overline{C_A}, \overline{C_B}, X, d, V_M)\end{aligned} \tag{8a}$$

$$\begin{aligned}\frac{d\overline{C_B}}{dx} &= \frac{\overline{\alpha_{B0}}\,\overline{\alpha_{A2}} - \overline{\alpha_{A0}}\,\overline{\alpha_{B2}}}{\overline{\alpha_{B1}}\,\overline{\alpha_{A2}} - \overline{\alpha_{A1}}\,\overline{\alpha_{B2}}} \\ &= g(\overline{D_A}, \overline{D_B}, \overline{D_Y}, \overline{C_A}, \overline{C_B}, X, d, V_M)\end{aligned} \tag{8b}$$

In these equations, the convection velocity will be considered as a function of the common concentration, the counter-ion pair and the membrane, but constant through the DBLs and the IEM. The V_M values used in the calculations are those obtained experimentally for a typical system (NaCl/CM2/LiCl).[17]

In our procedure, we have to know the limiting conditions, that is the concentrations in the membrane at the interfaces. These are determined from the equilibrium condition between

the DBLs and the membrane using the Donnan equation, which leads to the two following equations:

$$K_{Aff} = \frac{\overline{C_A}}{C_A}\frac{C_B}{\overline{C_B}} \quad (9a)$$

$$K_{sel} = \frac{C_A}{\overline{C_A}}\frac{C_Y}{\overline{C_Y}} \quad (9b)$$

where K_{Aff} and K_{sel} are, respectively, the affinity coefficient and the selectivity coefficient.[9] These two coefficients present the ionic activity coefficient variations between the membrane and the solutions. In fact, if we introduce the coefficients K_A, K_B and K_Y defined by $K_i = (\gamma_i/\overline{\gamma_i})$, then eqn. (9a) and (9b) become:

$$K_{Aff} = \frac{\gamma_A\overline{\gamma_B}}{\overline{\gamma_A}\gamma_B} = \frac{K_A}{K_B} \quad (10a)$$

$$K_{sel} = \left(\frac{\overline{\gamma}_{AY}}{\gamma_A}\right)^2 = \frac{1}{K_A K_Y} \quad (10b)$$

By symmetry these equations can be written for the interfaces $x = 0$ and $x = d$.

Numerical solution of the two differential equations written for each phase (DBLa, IEM or DBLb) needs a set of initial conditions. So, we choose two values of J_A and J_B obtained from Fick's law by supposing that the three phases constitute only one continuous phase of thickness equal to $d + 2\delta$ separating the bulk solutions a and b. From these values of J_A and J_B we compute initial values of: (*i*) $C_A(0)$ and $C_B(0)$ by solving the two differential equations (8a) and (8b) in the DBLa; (*ii*) $\overline{C_A}(0)$ and $\overline{C_B}(0)$ from $C_A(0)$ and $C_B(0)$ by using the affinity and selectivity coefficients; (*iii*) $\overline{C_A}(d)$ and $\overline{C_B}(d)$ by solving the two differential equations (8a) and (8b) in the membrane; (*iv*) $C_A(d)$ and $C_B(d)$ from $\overline{C_A}(d)$ and $\overline{C_B}(d)$ by using again the affinity and selectivity coefficients; (*v*) $C_A(d + \delta)$ and $C_B(d + \delta)$ by solving again eqns. (8a) and (8b) in the DBLb.

We compare then the computed values of $C_A(d + \delta)$ and $C_B(d + \delta)$ to the initial imposed values, 0 and C_0, respectively. If the difference is large, we select other initial values of the fluxes J_A and J_B and repeat the procedure. This iteration can be made automatically (according to the Newton–Raphson algorithm), with respect to the difference between the initial and the computed flux values.

For the present study, the diffusion boundary layer thickness, δ, the ionic diffusion coefficients in the membrane, $\overline{D_i}$, the selectivity and the affinity coefficients, K_{sel} and K_{Aff}, and the fixed function sites concentration, X, are chosen arbitrarily but within the order of magnitude found in the literature. We have investigated the system KCl (C_0)/IEM/LiCl (C_0) for which we have collected a maximum of data and the values of the parameters. In addition, the 1:1 electrolyte pair, KCl and LiCl, has a great difference in their cation mobilities, leading to high values of the ion fluxes and bi-ionic potential.

Results and discussion

General shape of the curve $J_i = f(C_0)$

On Figs. 2*a* and 2*b*, we report the variations of the counter-ion and co-ion fluxes *vs.* the common concentration, which varies from 0.01 to 10 mol L^{-1}. The values of the parameters used in this computation are given in Table 1. The A^+, B^+ and Y^- diffusion coefficients are respectively 1.95×10^{-5}, 1.05×10^{-5} and 2.05×10^{-5} $cm^2\ s^{-1}$ (corresponding to the particular case K^+, Li^+ and Cl^-). From Fig. 2*a*, using real coordinates, we remark, for high concentrations ($C_0 \geqslant 1$ mol L^{-1}), that the ionic fluxes vary linearly with C_0. However, from Fig. 2*b* corresponding to the curves $J = f(\log C_0)$, it appears that for low concentrations ($C_0 \leqslant 1$ mol L^{-1}): (*i*) the flux variations are asymptotic, decreasing to zero as C_0 tends to zero and (*ii*) the co-ion flux ($J_Y = J_A - J_B$), must be considered as negligible, and not of the same order of magnitude as the counter-ion flux. However, the co-ion flux is of the same order of magnitude as the counter-ion fluxes for $C_0 \geqslant 1$ mol L^{-1}. We also observe over the entire concentration range that the higher the mobility of the counter-ion, the higher its flux.

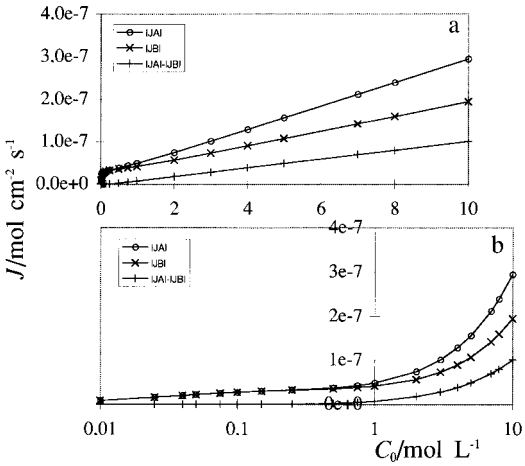

Fig. 2 Variation of (○) A^+, (×) B^+ and (+) co-ion fluxes *vs.* the common concentration: (a) linear coordinates, (b) semi-logarithmic coordinates.

The set of experimental results, obtained recently by Dieye and colleagues,[13,18] concerning the application of Donnan dialysis for defluorinating drinking water using anion-exchange membranes (AEM), confirm our previsions on the general shape of the curves $J_{counter\text{-}ion} = f(C_0)$. In fact, even if Dieye's experimental conditions are different from those corresponding to the proposed theoretical treatment (existence of a concentration gradient through the membrane, different counter-ions and co-ion nature, different membrane nature and characteristics, *etc.*) we observe, for the three AEM used (Fig. 3) small variations of the counter-ion fluxes for low concentrations followed by a very sharp increase for high concentrations. The single difference rests in the limits of the concentration domains, which are lower for Dieye's results, and are a function of the factors enumerated previously. In addition, the verification of the analytical equations, established in the absence of water flow and only for the two concentration domains (low and high), leads to the same conclusions concerning the phase that controls the interdiffusion process:[19] the DBL for low concentrations and the IEM for high ones.

Study of each parameter

In this section, we will study the influence of one parameter if we take all the others constant and equal to their values listed

Table 1 Parameter values used in the compilation of the ionic fluxes

Parameter	Value used
$D_K/cm^2\ s^{-1}$	1.95×10^{-5}
$D_{Li}/cm^2\ s^{-1}$	1.05×10^{-5}
$D_{Cl}/cm^2\ s^{-1}$	2.05×10^{-5}
$d/\mu m$	135
$\delta/\mu m$	60
$X/mol\ mL^{-1}$	1.66
$V_M/cm\ s^{-1}$	0
K_{Aff}	1
K_{sel}	1

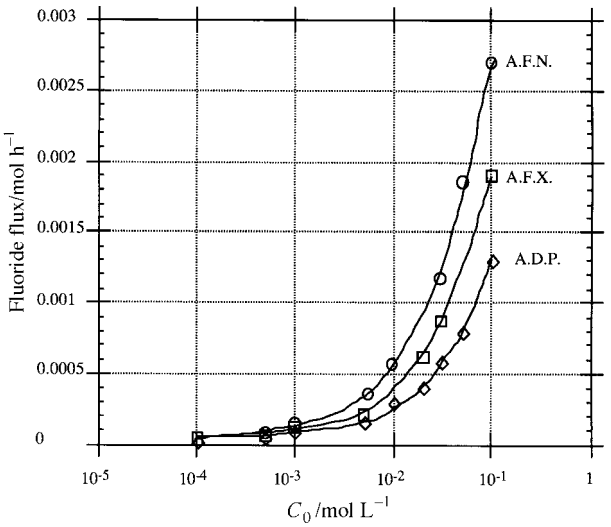

Fig. 3 Fluoride flux *vs.* the upstream compartment concentration for different membranes.[18]

in Table 1. The tested parameter will vary arbitrarily within a range fixed from the literature data.

Diffusion boundary layer thickness and the selectivity coefficient. To evaluate the DBL thickness influence on the different flux values, we have computed these fluxes for different values of δ at different common concentrations. The results obtained (Fig. 4) show the existence of two concentration domains: $C_0 \leqslant 0.1$ mol L^{-1} and $C_0 \geqslant 1$ mol L^{-1}. For $C_0 \leqslant 0.1$ mol L^{-1}, the asymptotic evolution of the A^+ flux *vs.* C_0 depends sharply on the δ values (Fig. 4a). The higher the DBL thickness, the faster the rate of decrease of J_A with concentration. For $C_0 \geqslant 1$ mol L^{-1}, we observe (Fig. 4b) that the evolution of the A^+ flux *vs.* C_0 is linear.

To study thoroughly the influence of the DBL thickness on the counter-ion flux, we present in Fig. 5 (curve *a*) the variation of the difference ΔJ_A between the fluxes corresponding to the two limiting values of the diffusion boundary layer thickness ($\delta = 60$ μm and $\delta = 200$ μm) *vs.* the common concentration C_0. We note that for low concentrations, up to $C_0 = 0.1$

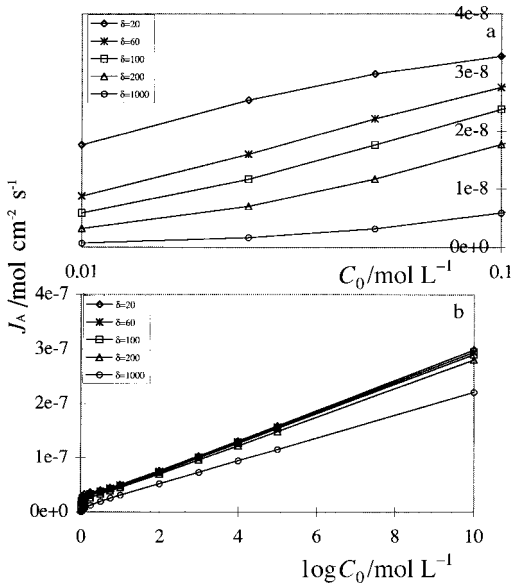

Fig. 4 Counter-ion flux *vs.* common concentration for different diffusion boundary layer thicknesses δ (in μm). (a) low values of C_0; (*b*) all values of C_0.

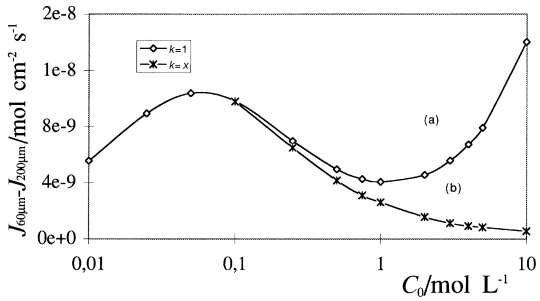

Fig. 5 The variation of the difference in the A^+ flux at $\delta = 60$ and 200 μm, *vs.* the common concentration [with K_{sel} equal to 1 (curve *a*) or variable (curve *b*), see Table 2].

mol L^{-1}, the difference ΔJ_A increases; it then decreases between 0.1 and 1 mol L^{-1}, and then again increases above $C_0 = 1$ mol L^{-1}. For weak concentrations, the value of the DBL thickness influences directly the evolution of the flux. The difference ΔJ_A increases from 0 to 10^{-8} mol cm^{-2} s^{-1}. For intermediate concentrations, this difference diminishes to 0.4×10^{-9} mol cm^{-2} s^{-1}, which corresponds to a non-negligible role of the IEM in the control of the interdiffusion process. It is well-known[9] that the higher the common concentration, the greater the role of the membrane in this control. However, for $C_0 \geqslant 1$ mol L^{-1}, ΔJ increases sharply. This is related to the decreasing influence of the DBL on the ionic fluxes.

To explain the shape of curve *a* presented in Fig. 5, we have to take into account the sorbed electrolyte, which can be quantified by the selectivity coefficient (eqn. 9b). In our computation, we have considered the experimental values of K_{sel} obtained by Belaid[20] using an atypical homogenous IEM membrane (CM2 from Tokuyama Soda) and NaCl electrolyte (Table 2). The results are given on the same figure (Fig. 5, curve *b*). In this case for $C_0 \geqslant 0.1$ mol L^{-1}, we remark a continuous decrease of the difference between the counter-ion fluxes corresponding to $\delta = 60$ μm and $\delta = 200$ μm. It appears that (*i*) the influence of DBL thickness decreases with the common concentration C_0 and (*ii*) the selectivity coefficient plays an important part at high concentrations, but not at low ones.

Co-ion diffusion coefficient in the membrane. On Fig. 6 we report the counter-ion flux variation *vs.* the common concentration for different co-ion diffusion coefficients in the membrane, varying from 10^{-7} to 5×10^{-7} cm^{-2} s^{-1}. For low concentrations, there is no influence of the co-ion diffusion coefficient on the counter-ion flux values. However, for high concentrations, this influence is very important and increases with concentration. In all cases, the increase of the co-ion diffusion coefficient implies an increase in the counter-ion flux differences, but the K^+ flux always remains higher than the Li^+ flux. We can explain these results by the fact that at low concentrations, the co-ion is almost completely excluded from the membrane, thus its $\overline{D_i}$ does not contribute to the ion flux.

Table 2 Experimental values of the sorbed electrolyte quantity (in microequivalents) and the selectivity coefficients obtained with a CM2 membrane and NaCl electrolyte[20]

C_0/M	n_{Cl}	K_{sel}
1.0	11.80	6.53
0.8	9.20	5.41
0.2	2.04	1.56
0.1	0.96	0.83
0.05	0.46	0.43
0.02	0.18	0.18
0.01	0.09	0.09

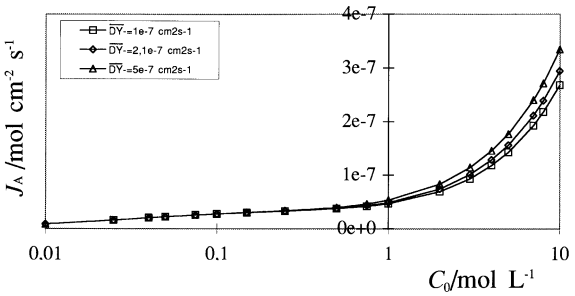

Fig. 6 Variation of the A^+ flux *vs.* the common concentration for different co-ion diffusion coefficients in the membrane.

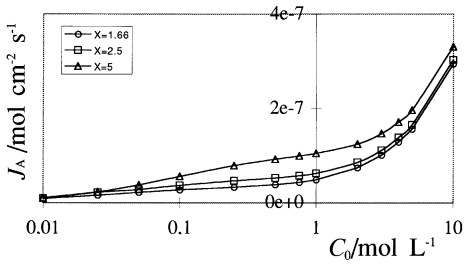

Fig. 8 Variation of the A^+ flux *vs.* the common concentration for different fixed site concentrations.

The A^+ counter-ion diffusion coefficient. In this paragraph, we discuss the influence of a counter-ion diffusion coefficient (for example $\overline{D_A}$) on the ionic fluxes (see Table 1). $\overline{D_A}$ has been varied from 10^{-7} to 10^{-6} cm^2 s^{-1} and the obtained results are reported in Fig. 7. Two concentration ranges are observed: at low concentrations, the co-ion flux is negligible and the interdiffusion process is entirely controlled by the diffusion boundary layers, while at very high concentrations, the influence of $\overline{D_A}$ is very important; the higher $\overline{D_A}$ the higher the flux of the counter-ion A and the higher the co-ion flux.

Fixed site concentration. In this study of the influence of the fixed site concentration, X, we have computed the ionic fluxes for different values of X: 1.66, 2.50 and 5.00 mole per liter of wet membrane in H^+ form. The results are reported in Fig. 8. We observe the existence of three different ranges of the common concentration C_0. For very low or very high values of C_0, the fixed site concentration influence on the ion fluxes is not very important. At low concentrations, the DBL controls the interdiffusion process. Then the membrane plays no part. At high concentrations, the electrolytes AY and BY penetrate considerably into the membrane and their concentrations become very high compared to X. Then, the fixed site concentration does not influence the diffusion of ions. At intermediate concentrations, this influence on all the ion fluxes is obvious, because the interdiffusion process is controlled by both the ion-exchange membrane and the diffusion boundary layers. For all curves, we note that the higher the value of X the higher the ionic flux, because the A^+ and B^+ concentration gradients in the membrane and in the DBLs increase with X.

Affinity coefficient. To study the affinity coefficient K_{Aff} influence on the ionic flux, we have used our treatment to compute these fluxes for different values of K_{Aff} (1, 1.5 and 2). These values are chosen to be as near as possible to the usual range of affinity coefficients corresponding to alkaline chloride electrolyte pairs.[21] We show on Fig. 9, the ionic flux variations *vs.* the common concentration and the affinity coefficient. It appears that for all concentration domains, the counter-ion flux variations are negligible.

Convection velocity. In Table 3 we give the variation of the A^+ counter-ion flux *vs.* the common concentration and the convection velocity V_M. The second column corresponds to a zero value of V_M. Column 4 corresponds to the computed A^+ fluxes taking into account the experimental values of V_M (column 3) given by Dammak *et al.*[22] for the bi-ionic system NaCl/CM2/LiCl, and only for C_0 less than 1 mol L^{-1}. The

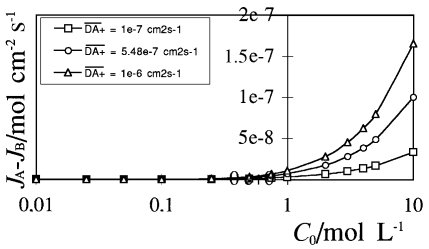

Fig. 7 Variation of the co-ion flux *vs.* the common concentration for different values of the diffusion coefficient of the counter-ion A^+ in the membrane.

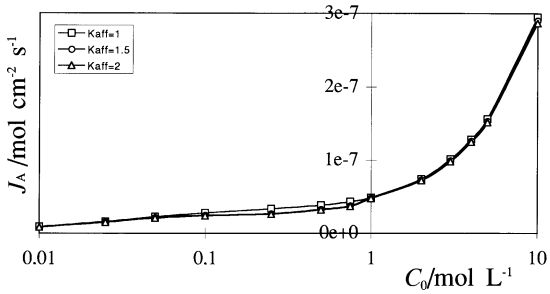

Fig. 9 Variation of the A^+ flux *vs.* the common concentration for different values of the affinity coefficient.

Table 3 Variation of the A^+ flux *vs.* the common concentration and the convection velocity V_M.

C_0/M	$J_A/10^{-8}$ mol cm^{-2} s^{-1}	$V_M/10^{-6}$ cm s^{-1}	$J_A/10^{-8}$ mol cm^{-2} s^{-1}	$J_A/10^{-8}$ mol cm^{-2} s^{-1} [a]
0.01	0.8743	0	0.8743	0.8743
0.025	1.5953	0	1.5953	1.5953
0.05	2.2077	0	2.2077	2.2077
0.1	2.7471	−0.30	2.7555	2.8312
0.25	3.3002	−0.75	3.3209	3.5091
0.5	3.7974	−1.37	3.8262	4.0896
1	4.8797	−1.31	4.88122	4.8983

[a] For $10 \cdot V_M$.

comparison of the two data sets leads us to assume that to the water transport contribution in the cross-ionic fluxes is negligible (less than 1%). However, for the bi-ionic potential, the convection velocity has a contribution of 6–7% of the BIP values. These same proportions can be obtained for convection velocities ten times higher than those obtained experimentally (column 5).

Conclusion

We have proven the important influence of the selectivity coefficient (K_{sel}) for mean and high concentrations, but the affinity coefficient plays a negligible part. We have also discussed the role of the membrane and the diffusion boundary layers, and presented a useful abacus for $J = f(\overline{D_Y})$ to determine the experimental values of $\overline{D_Y}$ under different experimental conditions (membranes, electrolytes, *etc.*). We confirm that the DBLs control the interdiffusion process at low concentrations, but at higher ones the process is controlled by the membrane. In the intermediate concentration domain, control of the interdiffusion process is mixed.

All these theoretical previsions will be verified experimentally and will be the subject of a future paper.

References

1 N. Lakshminaraynaiah, *Transport Phenomena in Membranes*, Academic Press, New York, 1969.
2 G. Scatchard and F. Helfferich, *Disc. Farad. Soc.*, 1956, **21**, 70.
3 K. Inenaga and N. Yochida, *J. Membrane Sci.*, 1980, **6**, 271.
4 K. Kaibara and H. Kimizuka, *Bull. Chem. Soc. Jpn.*, 1982, **55**, 1743.
5 D.Mackay and P. Meares, *Kolloidn Zh.*, 1959, **167**, 31.
6 M. Tasaka, H. Sugioka, M. Kamaya, T. Tanaka, S. Suzuki and Y. Ogawa, *J. Membrane Sci.*, 1988, **38**, 27.
7 M. Tasaka, S. Iwaoka, K. Yamagishi and Y. Ikeda, *J. Membrane Sci.*, 1985, **24**, 29.
8 A. Guirao, S. Mafé, J. A. Manzanares and J. A. Ibanèz, *J. Phys. Chem.*, 1995, **99**, 3387.
9 F. Helfferich, *Ion Exchange*, McGraw-Hill, New York, 1962.
10 T. Ktari and B. Auclair, *J. Membrane Sci.*, 1987, **32**, 251.
11 L. Dammak, C. Larchet, V.V. Nikonenko, V.I. Zabolotsky and B. Auclair, *Eur. Polym. J.*, 1996, **32**, 1199.
12 R. Schlögl and U. Schodel, *Z. Phys. Chem.*, 1955, **5**, 372.
13 A. Dieye, PhD Thesis, Université de Paris XII, 1995.
14 K. Bunzl, *J. Chem. Soc., Faraday Trans. 1*, 1993, **89**, 107.
15 L. Dammak, C. Larchet and B. Auclair, *J. Membrane Sci.*, in press.
16 F. G. Donnan, *Chem. Rev*, 1925, **1**, 73.
17 L. Dammak, PhD Thesis, Université de Paris XII, 1996.
18 A. Dieye, C. Larchet, B. Auclair and C. Mar-Diop, *Eur. Polym. J.*, 1998, **34**, 67.
19 A. Dieye, C. Larchet, B. Auclair and C. Mar-Diop, *Eur. Polym. J.*, 1999, **35**, 461.
20 N. N. Belaid, PhD Thesis, Université de Paris XII, 1993.
21 H. Miyoshi, M. Yamagami and T. Kataoka, *Chem. Express*, 1990, **10**, 717.
22 L. Dammak, R. Lteif, C. Larchet and B. Auclair, *New J. Chem.*, 1998, **22**, 605.

Paper 8/09931F